

Numerical Study of Coal Dust Explosions in Spherical Vessels

G. Continillo*

School of Engineering
University of California, Irvine
Irvine, California 92717

The unsteady flame propagation through a coal dust-air suspension in a spherical enclosure is studied by means of a one-dimensional, spherically-symmetric mathematical model. An Eulerian formulation is adopted for the gas phase mass continuity, species and energy balance equations, while a Lagrangian formulation is employed for the mass, energy and momentum balance equations for the particles. The pressure is assumed to be uniform in space (low Mach number) but varies in time. Preliminary calculations have been performed with a very simple coal particle submodel, in which a single-step devolatilization reaction with Arrhenius-type kinetics and quasi-steady heat, mass and momentum transfer to/from the particles is considered. Coal dust-air flame propagation could be predicted on the basis of devolatilization and homogeneous combustion reaction only. The model can represent a useful framework for the development and validation of particle-scale models, to be implemented in more complex coal combustion situations.

INTRODUCTION

The occurrence of dust explosions can be reconducted to the ability of a dust suspension to be ignited and to sustain a flame front propagating through it. To study the behavior of such systems is a difficult task due to the complex chemical and transport phenomena involved both in accidental explosions and in the controlled combustion of pulverized fuels. A look at the literature on dust explosions reveals substantial disagreement between the experimental results of the various authors, as pointed out by Hertzberg et al. (1). No comprehensive theory is available to explain the phenomenon and arguments are still being made about which is the dominant mechanism. In fact, the flame propagation through a flammable dust cloud can be predicted on the basis of different and even mutually excluding simplified models. For example, Essenhigh and Csaba (2) presented a model of coal dust flame propagation based on the incoming radiating heat from the walls to the particles, neglecting any other form of heat transfer and even the contribution of the combustion reaction. On the other hand, Smoot (3) proposed a coal dust flame model in which the conductive heat transfer is assumed to be the dominant mechanism. However, the experimental situations are still too complicated to be modelled in full detail, thus making quantitative comparison between experiment and theory almost impossible. The ignition and flame propagation in a cold dust suspension requires heat to be transferred from the burning mixture to the neighboring fresh mixture. Mitsui and Tanaka (4) modelled the propagation of a flame in an idealized cloud of particles. The ignition of a particle was assumed to take place at the surface, by heterogeneous combustion, as in Cassel and Liebman (5). Once ignited, an envelope flame was assumed to establish, due to the devolatilization, at a certain somewhat arbitrary distance from the surface and with a certain assigned flame temperature; then the unsteady spherically symmetric heat conduction equation was solved to calculate the temperature in the gas phase surrounding the burning particle. Flame propagation was stated to be possible when the temperature at the location of the adjacent particle reached the ignition temperature before than the envelope flame

* On leave from: Istituto Ricerche sulla Combustione, Consiglio Nazionale delle Ricerche, Naples, Italy

extinguished for the volatile fuel consumption of the first particle. This idealized situation is still amenable of analytical treatment; particle-air relative motion, density and pressure variation, unsteady particle heat up and pyrolysis cannot be introduced without making the analytical solution impossible.

When a numerical solution is considered, the model can be complicated almost unlimitedly. The literature shows that the tendency has been either to refine the model for a single particle, with a very idealized environmental situation (for example Kansa and Perlee (6)) or to study very complicated flow situations like industrial burners, as in the works reviewed by Smoot (7). Both these approaches do not offer a direct contribution to the understanding of the dominant mechanisms of flame propagation in dust explosions, the first because of the poor or non-existing consideration of the particle-gas and particle-particle interactions, the second because of the impossibility of giving a close description of the particle scale phenomena at the same time of describing large scale, complicated flow and heat transfer patterns.

Aim of the present work is to identify a model problem in which the parameters are not too many, and fairly controllable, with a simple geometry and flow field, so that more computational efforts can be devoted to the microscale phenomena. The problem is meant to be still representative of a conceivable practical situation, like the deflagration in a spherical enclosure. The framework is presented in this paper, and preliminary calculations, with the inclusion of a simplified model for the unsteady particle heat-up and pyrolysis, are performed. Some of the results are shown and discussed, and further developments are indicated in the foregoing.

MATHEMATICAL FORMULATION

Gas Phase Model. The gas phase model is essentially that of Reference (8), in which liquid spray flames were investigated. The following main assumptions are made. The flow is one-dimensional, unsteady, laminar, spherically symmetric. The viscous dissipation rate is negligible and the pressure is constant along the space coordinate (low Mach number), but varies in time due to the confinement in the vessel. The gas mixture is thermally perfect. Binary diffusion coefficients for each pair of species are taken to be equal, thermal mass diffusion is neglected. Mass diffusion and heat conduction are governed by Fick's and Fourier's law, respectively. The diffusion coefficient is assumed to vary with temperature and pressure ($\rho D = \mu = \text{constant}$). The Lewis number is unity. Radiative heat transfer is neglected. The combustion chemistry is described by means of a single-step, irreversible reaction of the volatiles with the oxygen; Arrhenius-type kinetics with non-unity exponents for fuel and oxygen concentrations, as proposed by Westbrook and Dryer (9), is included. The equations include coupling terms accounting for mass, momentum and energy exchanges between the two phases.

The dimensional unknown quantities and the variable physical parameters are nondimensionalized with respect to their initial values, except that for the velocity. The following reference quantities are defined: $r_c = R$; $t_c = R^2/D_0$; $u_c = D_0/R$, where r is the space coordinate, R is the radius of the enclosure, t is the time coordinate, D_0 is the diffusion coefficient at a reference temperature, u is the gas velocity; furthermore, the nondimensional number density of the (k)th particle group $n_k = n'_k R^3$, the nondimensional heat of combustion $Q = Q'/C_p T_0$ and mass production rate for the (i)th species $\dot{w}_i = \dot{w}'_i (R^3/\rho_0 D_0)$ are defined, where ρ_0 is the gas density evaluated at the initial temperature and pressure, and the following nondimensional equations are derived.

Continuity:

$$\frac{\partial \rho}{\partial t} + \frac{1}{r^2} \frac{\partial}{\partial r} (r^2 \rho u) = - \sum_{k=1}^N n_k \dot{m}_k \quad 1)$$

where \dot{m}_k is the mass devolatilization rate of the (k)th particle group, N is the total number of particle groups.

Species:

$$\rho \frac{\partial Y_j}{\partial t} + \rho u \frac{\partial Y_j}{\partial r} - \frac{1}{r^2} \frac{\partial}{\partial r} (r^2 \frac{\partial Y_j}{\partial r}) = (\delta_{jF} - Y_j) \sum_{k=1}^N n_k \dot{m}_k + \dot{w}_j \quad 2)$$

where Y_j is the (j)th species mass fraction, δ is the Kroneker delta, and the subscript F stays for "vapor fuel."

Energy:

$$\rho \frac{\partial \phi}{\partial t} + \rho u \frac{\partial \phi}{\partial r} - \frac{1}{r^2} \frac{\partial}{\partial r} (r^2 \frac{\partial \phi}{\partial r}) = - \frac{p}{C_p} \left(\frac{C_p T}{C_{p0} T_0} \right) \sum_{k=1}^N n_k \dot{q}_k + Q \dot{w}_F \quad 3)$$

with

$$\phi = T p^{\frac{1-\gamma}{\gamma}} = T p^\Gamma$$

where p is the pressure, C_p is the specific heat at constant pressure, T is the temperature, the subscript p stays for "particle", and q_k is the heat flux coming from one particle belonging to the (k)th group (usually negative), whose expression will be given later.

Ideal gas state equation:

$$p = \rho T \quad 4)$$

Velocity (integrating Eq. 1 over $r^2 dr$) is given by:

$$u = \frac{1}{\rho r^2} \int_0^r \left(\sum_{k=1}^N n_k \dot{m}_k - \frac{\partial \rho}{\partial t} \right) r^2 dr \quad 5)$$

Pressure (integrating Eq. 1 over $r^2 dr$ between 0 and R) is given by:

$$\left[\int_0^1 \frac{r^2 dr}{T} \right] \frac{dp}{dt} + \left[\frac{\partial}{\partial t} \int_0^1 \frac{r^2 dr}{T} \right] p = \int_0^1 \sum_{k=1}^N n_k \dot{m}_k r^2 dr \quad 6)$$

The initial and boundary conditions for the gas phase are:

$$Y_j(r,0) = Y_{j0} ; u(r,0) = 0 ; \phi(r,0) = 1 ; p(0) = 1 \quad 7)$$

$$\left. \frac{\partial Y_j}{\partial r} \right|_{r=0} = 0 ; \left. \frac{\partial Y_j}{\partial r} \right|_{r=1} = 0 ; \left. \frac{\partial T}{\partial r} \right|_{r=0} = 0 ; \left. \frac{\partial T}{\partial r} \right|_{r=1} = 0 \quad 8)$$

$$u(0,t) = u(1,t) = 0$$

Particle Model. In the calculations presented in this paper, the transient behavior of a particle is described by means of an extremely simplified model. The coal particle is represented by a sphere of solid material (ashes and fixed carbon) and volatiles in a specified initial partition. The particle is

considered to remain spherical and conserve its volume. The temperature is considered uniform in the particle and on the particle surface. Following Hubbard et al. (10), the transport processes next to the particle (in the "film") are assumed to be quasi-steady, and the thermophysical properties of the air-fuel vapor mixture are assumed uniform and evaluated at a conveniently averaged value of the temperature in the film. The fuel vapor production rate is assumed to depend on the particle temperature and global composition only. During the particle heat-up, the volatiles are released according to a simple one-step Arrhenius pyrolysis reaction, as in (6). The surface oxidation reaction is not considered, due to the highly transient character of the particle history in this kind of phenomena. This eliminates the need for considering the mass transfer processes in the film: all of the volatiles released by the particle are immediately available in the gas phase. The model accounts for the effects of the convective transport caused by the gas-particle relative motion by means of correction factors to the spherically symmetric stagnant film situation.

The non-dimensional equations for each particle group are:

Volatiles:

$$\frac{dm_v}{dt} = -A_v \exp(-T_v/T_p) m_v \quad (9)$$

where m_v is the mass of volatiles, $A_v = A'_v R^2/D_0$ is a non dimensional preexponential factor, T_v is a non dimensional activation temperature.

Momentum:

$$\frac{dv}{dt} = \frac{N_1}{8} \text{Re} C_D (u - v) \frac{\rho_\infty}{\rho_p} \quad (10)$$

$$\text{with } N_1 = \frac{3}{2} \frac{R^2}{a^2} \quad \text{and (11): } C_D = \frac{24}{\text{Re}} \left(1 + \frac{1}{6} \text{Re}^{2/3}\right) \quad (11)$$

where v is the particle velocity, Re is the Reynolds number, the subscript ∞ stays for "free stream conditions" referring to a particle, a is the radius of the particle.

Energy:

$$\frac{dT_p}{dt} = N_1 \frac{C_p}{C_{pp}} \text{Nu} (T_\infty - T_p) \frac{\rho_\infty}{\rho_p} \quad (12)$$

$$\text{with (12)} \quad \text{Nu} = 2 + 0.6 \text{Re}^{1/2} \text{Pr}^{1/3} \quad (13)$$

where Pr is the Prandtl number. The instantaneous position of particle group k is given by

$$\frac{dr_k}{dt} = v_k \quad (14)$$

The free-stream values of temperature and velocity are those of the gas phase model equations, evaluated at the current particle location. Finally, for the source terms in Eqs. 1, 2, and 3, we have:

$$\dot{m}_k = -\left(\frac{dm}{dt}\right)_k \quad (15)$$

$$\dot{q}_k = \frac{C_{po}}{C_{pp}} \left[3 \frac{\rho_o}{\rho_{po}} \frac{R^2}{a^2} \text{Nu} + \beta \sqrt{v_k} C_p \right] (T_{pk} - T) \quad (16)$$

where ρ_{po} is the initial density of the particle, and $\beta_v = \rho_{vo}/\rho_{po}$ is the initial mass fraction of volatiles in the particles.

For the numerical solution, gas phase and particle calculations are time-split. The source terms provided by the particle calculations for the (n)th time level are used in the (n + 1)th time level of the gas phase calculations, after proper interpolation, and so forth. Explicit finite difference schemes are employed to discretize the PDEs of the gas phase model - except that for the chemical production terms, for which a degree of implicitness is introduced - since they have been proved to be the most effective in such two-phase problems (13). A non-uniform spatial grid is used, with the finest mesh size next to the wall. The time step is dynamically changed in order to describe the evolution of the system according to the current time scale. Due to the coupling of the equations, the calculations are iterated within each time step until the desired level of convergence is achieved. Then the integration in time is continued until desired.

RESULTS AND DISCUSSION

Ignition is achieved by means of a heat source in the energy equation, in a spherical region for a limited time and an assigned intensity. The model predicts the particle heat-up, the devolatilization and the ignition of the volatiles in the gas phase, and the flame propagates through all the volume. The values of the parameters used for the base case are listed in Table I.

Table I.

Values and Expressions Used for the Most Important Physical Parameters in the Base Case

a	- 2.5x10 ⁻⁵ m	R	- 5x10 ⁻² m
A _v	- 1.x10 ⁷ s ⁻¹	T _o	- 3x10 ² K
C _p	- 1.01x10 ³ + 1.95x10 ⁻¹ (T'-300) J/KgK	T _v	- 15000/R K
m _{vo} / m _{po}	- 0.25	γ	- C _p /(C _p - R)
P _o	- 1x10 ⁵ Pa	μ _o	- 1.845x10 ⁻⁵ Kg/ms
Q	- 4.421x10 ⁷ J/Kg	ρ _{po}	- 1.36x10 ³ Kg/m ³

Figure 1 shows the computed pressure-time patterns for different particle diameters. The predicted final pressure, close to the maximum theoretical adiabatic pressure achievable, is much higher than that found in the experiments. The reasons are that the model does not account for heat losses, nor for the endothermic dissociation in the burned mixture. A slight decrease is observed after the maximum, and this accounts for the cooling effect due to the residual solid particles. During the combustion, the rate of pressure rise is always increasing: this is in agreement with predictions of lumped parameter models and with results of the experiments for the part in which the heat losses are negligible (14). In fact, it has been shown by means of a two-zone, thin flame model (14) that the rate of pressure rise can be expressed as

$$\frac{dp}{dt} = \frac{3\gamma p}{R} \frac{Q_R}{C_v T_u} \left(\frac{r_f}{R}\right)^2 S_u \quad (17)$$

where Q_R is the heat of reaction per unit mass of gas, C_v is the specific heat at constant volume, T_u is the temperature of the unburned mixture, r_f is the current radial location of the flame, and S_u is a flame speed with respect to the unburned mixture. For Equation 17 all the information connected with the flame structure is included (and hidden) in the parameter S_u , like the transport phenomena, the combustion reaction rate, the particle-gas interactions (relative motion, thermal inertia of the condensed phase), the rate of pyrolysis. A distributed-parameters model like that of the present work is capable of resolving the flame structure, therefore it allows for an appreciation of the different behavior of dust suspensions for what all of the parameters in Eq. 17 are equal, except S_u . For example, the influence of the particle size is clearly seen in Fig. 1, where finer particles are shown to give rise to faster flame propagation. Figure 2 illustrates the influence of another parameter, namely the oxygen content of the suspending atmosphere; the initial solid concentration is chosen accordingly to be slightly more than stoichiometric, in order to avoid the presence of oxygen in the residual gases together with the residual solid particles, which would require the consideration of the solid-gas surface oxidation reaction, not included in the model at present. The maximum pressure obviously decreases with the content of reactants, since the total amount of heat released by the combustion reaction is lower; the duration of the explosion increases, the system showing a lower overall reactivity, as expected.

Figure 3 represents the spatial profiles of the main variables at successive times for the base case. Each circle represents one particle group, whose particles are distributed on a spherical surface: the abscissa of each one represents the current radial location, while the ordinate corresponds to the particle temperature, in the same scale as that of the gas temperature. The radius of the internal filled circle is proportional to the remaining fraction of volatiles. The ignition zone is rapidly heated to about 1500 K, while the particles remain at a temperature close to the initial. The heat provided by the ignition source is conducted towards the outer region, and to the particles in the ignition region, until they begin to pyrolyze. Note that the particles have a tendency to spread out, due to the motion impressed by the expanding gas during the ignition energy supply. This causes a local decrease of the volumetric concentration of dust, but the gas concentration has, of course, become even lower due to thermal expansion, therefore the overall effect is that of the generation of a locally fuel-rich region. When the vapor fuel released is sufficient, individual flames set up at the location of the particles, where the oxygen is seen to be consumed, and peaks in the temperature profiles appear. During the propagation of the flame, it is seen that the vapor fuel is present in the burned region only, meaning that it reacts as soon as it is generated. In fact the gas temperature is much higher than that of the particles when they begin to pyrolyze, up to the point that the combustion reaction is much faster than the pyrolysis, notwithstanding the much higher activation energy and the low concentration of the fuel vapor. Therefore, the limiting stage is the pyrolysis in this case. The relative motion of the two phases generates a deviation from the initially uniform, slightly richer than stoichiometric, equivalence ratio. More precisely, at the beginning the gas velocity is mainly directed towards the wall, and the particles, due to their kinematic inertia, do not follow the gas with the same velocity, thus creating a locally richer mixture in the center. The system is closed, thus a locally lean mixture is being generated in the zones encountered by the flame going towards the wall. When the flame approaches the wall, the gas velocity is mainly directed towards the center, while the particles are still moving towards the wall, and this generates a locally rich mixture next to the wall. As a result of the phenomenon, an uneven residual fuel vapor distribution is found at the end of the propagation.

CONCLUSIONS

A model problem for ignition and unsteady flame propagation in a coal dust-air suspension has been identified. The simple geometry and flow field allow for

more details to be included in the modelling of the microscale phenomena. The problem can be considered still representative of a practical situation like a deflagration in a spherical enclosure. Results obtained with the inclusion of a simplified model for the unsteady particle heat-up and pyrolysis have been presented and discussed, and qualitative agreement with experimental evidence and simpler theoretical approaches has been found. Coal dust-air flame propagation has been predicted on the basis of devolatilization and homogeneous combustion reaction only, although the range of variation of some parameters is currently limited by the approximations made in the simplified coal particle model. It has been demonstrated that the model can represent a useful framework for the development and validation of much more detailed particle-scale models, to be implemented in more complex coal combustion situations.

Acknowledgments

This work has been partly supported by the Consiglio Nazionale delle Ricerche, Italy, with a NATO-CNR scholarship for exchange visitors granted to the author. Professor William A. Sirignano is gratefully acknowledged for his kind hospitality, support and advice.

References

1. Hertzberg, M., Cashdollar, K.L., Opferman, J.J., "The Flammability of Coal Dust - Air Mixtures," Bureau of Mines, RI 8360 (1979).
2. Essenhigh, R.H., Csaba, J., Ninth Symp. (Int.) on Combustion, p. 111, The Combustion Institute, Pittsburgh, 1963.
3. Smoot, L.D., Horton, M.D., Prog. Energy Combust. Sci. 3, 235 (1977).
4. Mitsui, R., Tanaka, T., Ind. Chem. Eng. Process Des. Develop. 12, 384 (1973).
5. Cassel, M., Liebman, I., Combust. Flame, 3, 467 (1959).
6. Kansa, E.J., Perlee, H.E., Combust. Flame 38, 17 (1980).
7. Smoot, L.D., Prog. Energy Combust. Sci. 10, 229 (1984).
8. Continillo, G. and Sirignano, W.A., submitted to the Twenty-Second International Symposium on Combustion, Seattle, 1988.
9. Westbrook, C.K., Dryer, F.L., Prog. Energy Combust. Sci. 10, 1 (1984).
10. Hubbard, G.L., Denny, V.E., Mills, A.F., Int. J. Heat Mass Transfer 18, 1003 (1975).
11. Faeth, G.M., Prog. Energy Combust. Sci. 3, 191 (1977).
12. Ranz, W.E., Marshall, W.R., Jr., Chem. Eng. Prog. 48, 141 (1952).
13. Aggarwal, S.K., Fix, G.F., Lee, D.N., Sirignano, W.A., J. Comput. Phys. 35, 229 (1983).
14. Continillo, G., Study on Coal Dust Explosibility in Spherical Vessels, Doctoral Thesis, University of Naples, Naples, Italy, 1987 (in Italian).

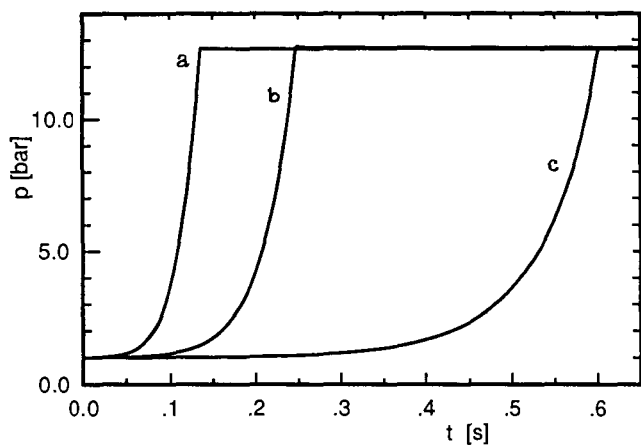


Figure 1. Pressure-time patterns at various particle diameters:
 a) 30 μm ; b) 50 μm (base case); c) 100 μm ;

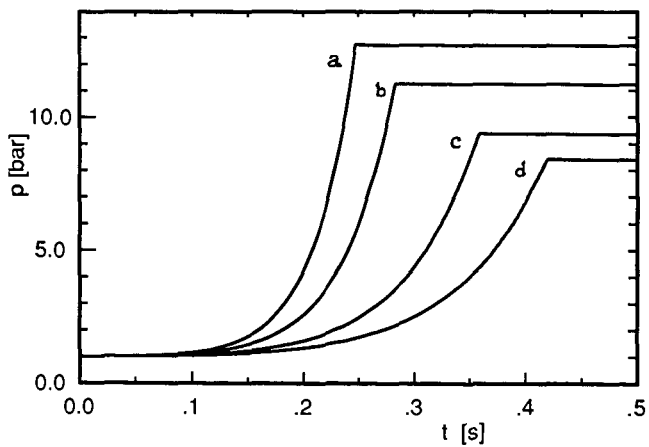


Figure 2. Pressure-time patterns at various oxygen mass fractions in the suspending atmosphere: a) 23.2% (base case); b) 20%; c) 16%, d) 14%

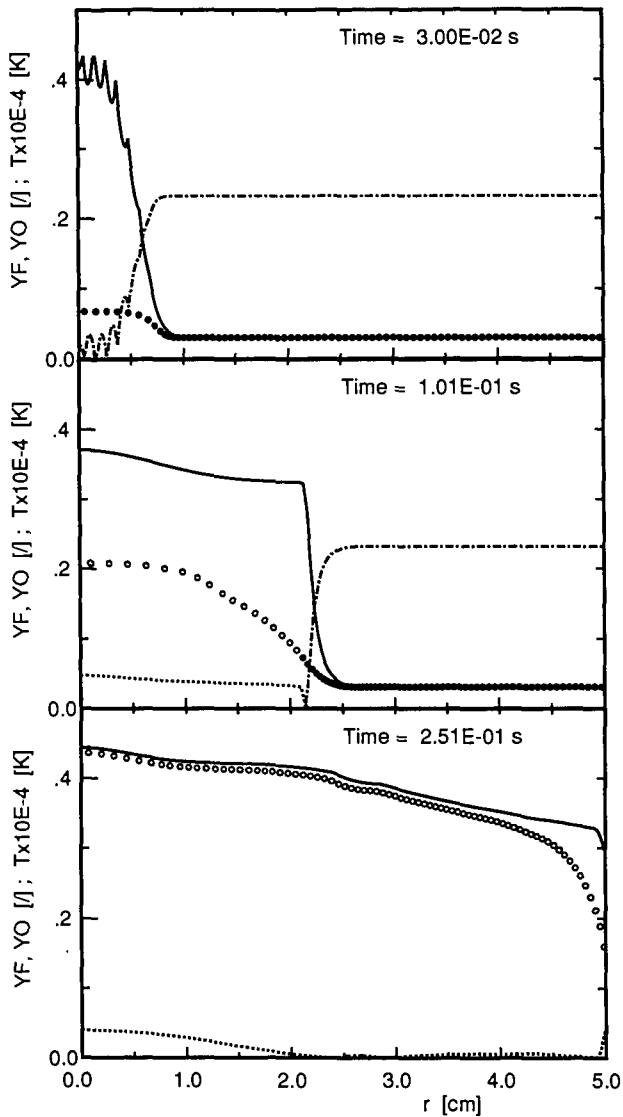


Figure 3. Radial profiles of fuel (YF, dashed) and oxygen (YO, dot and dash) mass fractions, and of temperature (T, solid line) at successive times.